

Evidence for dominant Pauli paramagnetic effect in the upper critical field of single-crystalline $\text{FeTe}_{0.6}\text{Se}_{0.4}$

Seunghyun Kim,¹ Jae Wook Kim,¹ Eun Sang Choi,² Yunkyu Bang,³ Minoru Nohara,^{4,5}
Hidenori Takagi,^{5,6,7} and Kee Hoon Kim^{1,6,*}

¹*CeNSCMR and Department of Physics and Astronomy, Seoul National University, Seoul 151-742, Republic of Korea*

²*NHMFL, Florida State University, Tallahassee, Florida 32310, USA*

³*Department of Physics, Chonnam National University, Kwangju 500-757, Republic of Korea*

⁴*Department of Physics, Okayama University, Okayama 700-8530, Japan*

⁵*TRIP, JST, 5 Sanbancho, Chiyoda, Tokyo 102-0075, Japan*

⁶*Department of Advanced Materials, University of Tokyo, Kashiwa, Chiba 277-8561, Japan*

⁷*RIKEN Advanced Science Institute, Wako, Saitama 351-0198, Japan*

(Received 22 January 2010; revised manuscript received 5 April 2010; published 14 May 2010)

We investigated the temperature dependence of the upper critical fields $H_{c2}(T)$ of a superconducting $\text{FeTe}_{0.6}\text{Se}_{0.4}$ single crystal by measuring its resistivity in static magnetic fields up to 45 T. Our observations of strong bending in the $H_{c2}^{ab}(T)$ curves and a nearly isotropic $H_{c2}^{ab}(0) \approx H_{c2}^c(0) \approx 48$ T support the presence of a strong Pauli paramagnetic effect. We show that the Werthamer-Helfand-Hohenberg formula that includes both the Pauli limiting and the spin-orbit scattering can effectively describe both the $H_{c2}^{ab}(T)$ and $H_{c2}^c(T)$ curves. An enhancement in the quasiparticle density of states or the increased scattering resulting from Te(Se) vacancies or excess Fe is discussed as a possible origin for the manifesting Pauli paramagnetic effect.

DOI: [10.1103/PhysRevB.81.184511](https://doi.org/10.1103/PhysRevB.81.184511)

PACS number(s): 74.70.-b, 74.72.-h, 74.81.Bd

I. INTRODUCTION

The observation of high-temperature superconductivity in iron pnictides has triggered a surge of research activity in recent years investigating their basic superconducting properties and pairing mechanism.¹ The upper critical field H_{c2} is one of the fundamental superconducting parameters that provides clues to the pairing mechanism as well as to the pairing strength. Moreover, the temperature dependence of H_{c2} , $H_{c2}(T)$, and its anisotropy reflect the underlying electronic structure and provide valuable information on the microscopic origin of pair breaking, which can, in turn, be important for application purposes.

In this respect, $H_{c2}(T)$ has been extensively studied in various forms of iron pnictide ranging from the “1111” system, represented as $RE\text{FeAsO}$ (RE =rare earth), to the “122” system, such as $A\text{Fe}_2\text{As}_2$ (A =alkali metal). Possibly because of the large fields required and the scarcity of single crystals, investigations of the 1111 system are still limited but have shown the existence of anisotropy between H_{c2} in an ab -planar field (H_{c2}^{ab}) and in a c -axis field (H_{c2}^c) near the superconducting transition temperature T_c .^{2–6} Moreover, H_{c2}^{ab} and H_{c2}^c increase almost linearly or sublinearly with decreasing temperatures near T_c , resulting in the maximum slope change: $-dH_{c2}^{ab}/dT_c|_{\text{max}} \sim 9\text{--}11$ T/K. These characteristics of H_{c2} curves support the presence of the multiband effect in the system. The 122 system also shows quite linear or sub-linear increases in H_{c2}^{ab} and H_{c2}^c as well as in their anisotropy near T_c , consistent with the multiband scheme. The maximum slope change ($-dH_{c2}^{ab}/dT_c|_{\text{max}}$) in the 122 system is much smaller than in the 1111 system, showing $\sim 3\text{--}6$ T/K.^{7–10} In the orbital-limiting scenario, the expected $H_{c2}^{ab}(0)$ can be as high as 150–300 T in the 1111 system, while it is about 80–120 T in the 122 system.

In reality, however, most of the existing data for the $H_{c2}^{ab}(0)$ in the 122 system are smaller than 60 T. This experi-

mental situation is also related to the fact that the anisotropy ratio between H_{c2}^{ab} and H_{c2}^c decreases with decreasing temperature in most of the iron pnictides.^{7–10} Thus, most 122 single crystals and thin films including both hole-doped $(\text{Ba},\text{K})\text{Fe}_2\text{As}_2$ and electron-doped $\text{Sr}(\text{Fe},\text{Co})_2\text{As}_2$ have shown nearly isotropic $H_{c2}(0)$ behavior. The existence of such an isotropic $H_{c2}(0)$ in 122 materials with a cylindrical Fermi surface is quite unusual and is in sharp contrast to the case of layered cuprates. Although band warping in the cylindrical surface and multiband effects have been discussed as possible origins of the isotropy, those mechanisms alone might not be enough to explain the existence of an isotropic $H_{c2}(0)$ that is insensitive to the doping level and the degree of disorder.

The iron chalcogenides, including $\text{Fe}(\text{Te},\text{Se})$, with PbO-type structures are yet another new type of Fe-based superconductor with $T_c = 8.0\text{--}14.5$ K.^{11–16} The structure of an iron chalcogenide is characterized by simple planar sheets of tetrahedrally coordinated Fe, which is common to the iron pnictide superconductors. The Fermi surface is composed of cylindrical hole and electron pockets, similar to those of the iron pnictides.^{17,18} In view of the similarities in electronic structure, the study of $H_{c2}(T)$ and its anisotropy in $\text{Fe}(\text{Te},\text{Se})$ systems is expected to provide useful comparisons to the 122 system and to elucidate the origin of the isotropic $H_{c2}(0)$. In the first attempt to investigate the $H_{c2}(T)$ in polycrystalline $\text{FeSe}_{0.25}\text{Te}_{0.75}$, a strong bending of the H_{c2} curve with decreasing temperature was observed, an indication of the Pauli paramagnetic effect.¹⁹ A subsequent measurement on a single crystal $\text{Fe}_{1.11}\text{Te}_{0.6}\text{Se}_{0.4}$ showed weak anisotropy in the $H_{c2}(0)$, which was interpreted as a possible band-warping effect, similar to the 122 case.²⁰

In this study, we have used static magnetic fields up to 45 T to determine the resistive $H_{c2}^{ab}(T)$ and $H_{c2}^c(T)$ curves of an $\text{FeTe}_{0.6}\text{Se}_{0.4}$ single crystal with unprecedented accuracy. We found that the system showed a nearly isotropic $H_{c2}(0)$ of

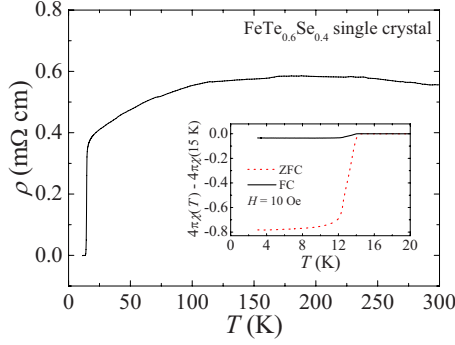


FIG. 1. (Color online) The temperature dependence of the resistivity of an $\text{FeTe}_{0.6}\text{Se}_{0.4}$ single crystal under a zero magnetic field in a broad temperature window. T_c is 14.5 K. Inset: the change in the dc magnetic susceptibility χ multiplied by 4π near T_c , relative to the value at 15 K, which was measured at $H=10$ Oe applied along the ab plane after field cooling (solid) and zero field cooling (dotted).

~ 48 T and a strong bending effect in $H_{c2}^{ab}(T)$. The details of the temperature dependence of H_{c2} curves can be successfully explained by the Werthamer-Helfand-Hohenberg (WHH) prediction, which considers both the Pauli-limiting effect and the spin-orbit scattering effect. Our results suggest that the Pauli-limiting effect could be the main source of the peculiar isotropic $H_{c2}(0)$ for this iron-chalcogenide superconductor.

II. EXPERIMENTS

Single crystals of $\text{FeTe}_{0.6}\text{Se}_{0.4}$ were grown by the self-flux method in an evacuated quartz tube. The mixture of Fe and (Te,Se) with a starting composition of $\text{Fe}(\text{Te}_{0.6}\text{Se}_{0.4})$ was heated at 1193 K for 12 h and slowly cooled down to room temperature afterwards at a rate of 40 K/h. The resistivity was measured down to 1.5 K by the standard four-probe method in a physical property measurement system (PPMS) up to 14 T and in a hybrid magnet (NHMFL, Tallahassee, USA) from 11.5 to 45 T. To prepare specimens for transport measurements, we first prepared a rectangular-shaped crystal ($3 \times 1 \times 0.6$ mm³) and cleaved the piece with a razor blade along the ab plane into the two pieces ($3 \times 1 \times 0.29$ mm³ and $3 \times 1 \times 0.30$ mm³). The resistivity measurements for the two pieces at zero magnetic field showed the same T_c within 0.01 K and almost identical temperature dependence. The absolute resistivity values of the two pieces were close to each other within 10% at overall temperatures, which is mainly caused by the errors in the geometry estimation. These observations ensured us that the two pieces had almost identical physical properties. The two pieces were loaded onto the sample platform for the PPMS or the hybrid magnet in order to measure their resistivity under magnetic fields applied parallel to the ab plane and the c axis, respectively.

III. RESULTS AND DISCUSSION

Figure 1 shows the temperature dependence of the resistivity and the magnetization. We noted that the resistivity of

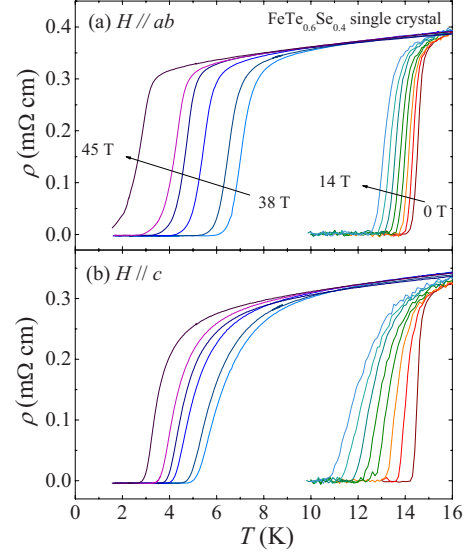


FIG. 2. (Color online) The temperature dependence of the resistivity from 0 to 14 T in 2 T increments and for 38, 39, 41, 42, 43, and 45 T along (a) the $H\parallel ab$ plane and (b) the $H\parallel c$ axis.

our samples showed the metallic behavior below approximately 200 K and showed superconductivity at 14.5 K, when determined from the criterion using 50% of the normal-state resistivity. The small transition width ($T_{\text{onset}} - T_{\rho=0}$) of about 1.3 K confirms the high quality of the crystal investigated. According to a recent study by Liu *et al.*,²¹ $\text{Fe}_{1.12}\text{Te}_{0.72}\text{Se}_{0.33}$ with a large amount of excess Fe shows semiconducting behavior down to the T_c , while $\text{Fe}_{1.04}\text{Te}_{0.72}\text{Se}_{0.28}$ with less Fe shows metallic temperature dependence. The amount of interstitial Fe existing between the FeTe(Se) layers is thought to be a decisive factor in causing this contrasting transport behavior. Therefore, the metallic resistivity in our sample suggests that our sample is close to stoichiometric $\text{Fe}(\text{Te}_{0.6}\text{Se}_{0.4})$ and has a minimal amount of excess interstitial Fe. Moreover, recent studies of transport and heat capacity^{15,16} in various Fe(Te,Se) samples revealed that a heat-capacity jump at T_c was observed only in the metallic samples with a diamagnetic volume fraction more than 75%, but not in the semiconducting samples. The magnetic susceptibility (χ) data of our sample (inset of Fig. 1) indeed show that a superconducting volume fraction is about 80%. Based on these experimental facts, i.e., metallic resistivity and large superconducting volume fraction, we thus infer that our sample has bulk superconductivity.

The temperature dependence of the resistivity under a static magnetic field is summarized in Fig. 2 for (a) $H\parallel ab$ and (b) $H\parallel c$. The temperature at which the zero resistivity was realized was systematically suppressed in an increasing magnetic field. The broadness of the transition was pronounced in the resistivity curves for $H\parallel c$, likely the result of enhanced, thermally activated vortex motion in this direction.⁸ Moreover, at $H < 14$ T, the transition into the superconducting state for $H\parallel ab$ occurred at higher temperatures than for $H\parallel c$, indicating H_{c2}^{ab} was higher than H_{c2}^c at temperatures near T_c . On the other hand, at $H=45$ T, the zero resistivity state was realized at 3.5 K for $H\parallel c$, which was slightly higher than the corresponding value for $H\parallel ab$,

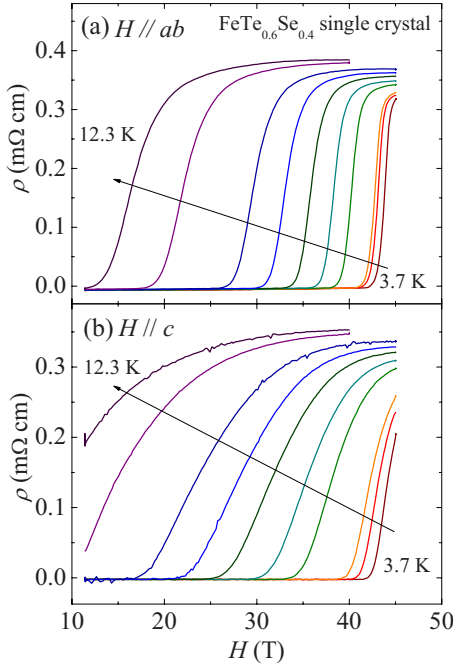


FIG. 3. (Color online) The magnetic field dependence of the resistivity at 3.7, 4.0, 4.5, 4.9, 5.9, 6.7, 7.9, 8.7, 9.7, 11.4, and 12.3 K along (a) the $H\parallel ab$ plane and (b) the $H\parallel c$ axis.

i.e., 2.8 K, indicating H_{c2}^c was very close to or even slightly higher than H_{c2}^{ab} near absolute zero temperature. The magnetic field dependence of the resistivity is also plotted from 38 to 45 T at several fixed temperatures in Fig. 3. Consistent with the behavior seen in the temperature dependence study, the transition width became broader for $H\parallel c$. Moreover, at $T=12.3$ K, the superconducting state was obviously more stable for $H\parallel ab$ than for $H\parallel c$, while at $T=3.7$ K, the transition into the normal state occurred at almost the same H .

We determined the temperature-dependent H_{c2}^{ab} and H_{c2}^c curves from the resistivity data summarized in Figs. 2 and 3. To determine the superconducting transition temperatures or fields from the resistivity, we used the criterion as the temperature where a 50% of normal-state resistivity just before entering the transition. With this criterion, we could minimize the effects of the vortex motion expected from the 10% criterion or the superconducting fluctuation expected from the 90% criterion. As shown in Fig. 4, the resultant H_{c2}^{ab} and H_{c2}^c curves from both field and temperature sweeps overlap each other, illustrating the consistency between the two experimental methods used to determine the H_{c2} curves.

The H_{c2} curves show anisotropic behavior near T_c , but become progressively isotropic as the temperature is lowered; $\gamma=H_{c2}^{ab}/H_{c2}^c$ is about 3 near T_c and 0.99 at $T=3.8$ K. Thus, it is likely that $H_{c2}(0)$ is nearly isotropic and reaches approximately 48 T. Therefore, our results clearly show that a nearly isotropic $H_{c2}(0)$ is realized even in our iron-chalcogenide superconductor, suggesting that this is a common physical feature in both 122 and “11” systems.^{7,9,20} In the former system, an isotropic $H_{c2}(0)$ was observed in both hole- and electron-doped single crystals, as well as in a thin film, indicating the isotropic behavior was less sensitive to the doping level and the degree of disorder. Combining pre-

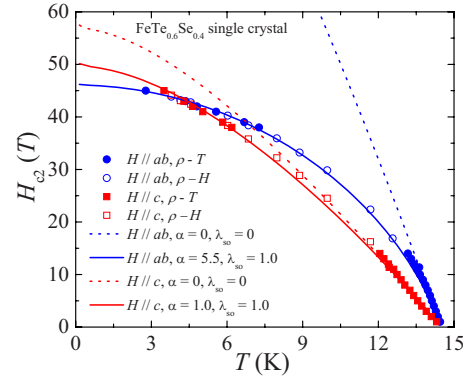


FIG. 4. (Color online) The $H_{c2}(T)$ curves for the $H\parallel ab$ plane and the $H\parallel c$ axis (symbols) determined using the criterion of 50% of the normal-state resistivity. The filled (open) symbols were taken from the temperature (magnetic field) dependence of the resistivity. The dotted lines represent the WHH prediction in which only orbital-limiting effects were considered ($\alpha=\lambda_{so}=0$). The solid lines indicate the best fits to the WHH curve with the parameters $\alpha=5.5$ and $\lambda_{so}=1.0$ for the $H\parallel ab$ plane and $\alpha=1.0$ and $\lambda_{so}=1.0$ for the $H\parallel c$ axis.

vious results in which a nearly isotropic $H_{c2}(0)$ was observed in an Fe-excessive crystal of $\text{Fe}_{1.11}\text{Te}_{0.6}\text{Se}_{0.4}$ (Ref. 20) and our present results in a more stoichiometric $\text{FeTe}_{0.6}\text{Se}_{0.4}$, it can be inferred that the isotropic H_{c2} property is also robust against variations in the Fe doping level. This observation strongly suggests that the isotropic $H_{c2}(0)$ property might not be a simple consequence of the three-dimensional band nature coming from the band-warping effect in the apparently cylindrical Fermi surfaces.

A worth noting feature seen in the $H_{c2}^{ab}(T)$ curves is the existence of a quite steep increase in the H_{c2} near T_c and the subsequent flattening of the curve at lower temperatures. The calculated maximum slope $-dH_{c2}^{ab}/dT|_{\text{max}} \sim 13$ T/K is the largest among the reported values for iron-based superconductors. This is a key feature that was also noticed by Kida *et al.*¹⁹ in the $H_{c2}(T)$ curve of a polycrystalline $\text{FeTe}_{0.75}\text{Se}_{0.25}$ sample. On the other hand, in a recent $H_{c2}^{ab}(T)$ study of a single-crystal $\text{Fe}_{1.11}\text{Te}_{0.6}\text{Se}_{0.4}$ specimen by Fang *et al.*,²⁰ the flattening feature in the $H_{c2}^{ab}(T)$ was not clearly identified, possibly because of the lack of data points near T_c . From the steeply increasing slope of H_{c2}^{ab} and H_{c2}^c curves in Fig. 4, we can calculate the orbital-limiting fields for each crystallographic direction. According to the WHH formula predicting the orbital-limiting field H_{c2}^{orb} for a BCS superconductor with a single active band,²² $H_{c2}^{\text{orb}}(0) = -0.69 dH_{c2}/dT|_{T=T_c}$, thus yielding $H_{c2}^{\text{orb}}(0) = 131.6$ T in $H\parallel ab$ and $H_{c2}^{\text{orb}}(0) = 56.5$ T in $H\parallel c$. These calculated values of $H_{c2}^{\text{orb}}(0)$ are much larger than the observed $H_{c2}(0)$ of approximately 48 T, suggesting that the low-temperature H_{c2} is predominantly a Pauli-limited upper critical field. The expected Pauli-limiting field for a weakly coupled BCS superconductor^{23,24} is estimated as $H_p(0) \equiv 1.86 T_c = 27.0$ T, which is much smaller than the predicted $H_{c2}^{\text{orb}}(0)$ as well as the experimental $H_{c2}(0) \approx 48$ T. This observation implies that the spin paramagnetic effect may play an important role in determining $H_{c2}(0)$ in this 11 system and that a mechanism to enhance the Pauli-limiting field beyond the BCS scenario might also be neces-

sary. On the other hand, recent scanning tunneling microscopy studies on stoichiometric Fe(Te,Se) crystals have reported that the gap energy Δ closely matches the BCS prediction of $2\Delta/k_B T_c \sim 3.5-3.8$. Thus, a simple scenario in which the system is in a strongly coupled non-BCS regime with a larger gap than that expected from the mean-field theory may not be adequate to explain the enhanced Pauli-limiting field.^{25,26}

Previously, several reports on the $H_{c2}(T)$ in Fe-based superconductors have shown that a two-band model in combination with orbital-limiting effects can effectively describe the overall curvature of H_{c2} .^{2,3,7,27,28} The main motivation for invoking the two-band model is to explain the almost linear or sublinear increase in the concave shape of the H_{c2}^c curve near T_c and its change to a convex form with decreasing temperature. However, in our case, both H_{c2}^{ab} and H_{c2}^c curves always exhibited a convex shape and the H_{c2}^{ab} curve flattened at temperatures below around $T_c/2$; none of these behaviors are compatible with the expected H_{c2} shape in the two-band system. Therefore, to describe the H_{c2} curves for the present iron chalcogenide, the spin paramagnetic effect and the orbital pair-breaking effect, but not necessarily the multiband effect, should be taken into account. It is expected that the Pauli limiting will be quite effective in explaining the isotropic $H_{c2}(0)$ limit while the orbital limiting can explain the anisotropy near T_c between H_{c2}^{ab} and H_{c2}^c curves.

With this motivation, we attempted to fit the experimental H_{c2} curves with the WHH formula that incorporates the spin paramagnetic effect via the Maki parameter α in a single-band system. Moreover, we also included the spin-orbit scattering constant λ_{so} in the fitting.²² For $H\parallel ab$, the attempt to fit the data without the Pauli paramagnetic effect, i.e., $\alpha=0$, only explained the experimental $H_{c2}(T)$ curve near T_c and showed clear deviations at low temperatures (dotted line in Fig. 4). The best fit was obtained when $\alpha=5.5$ and $\lambda_{so}=1.0$. The large value of $\alpha=5.5$ is comparable to that for CeCoIn₅ and organic superconductors that have shown the first-order transition in H_{c2} , forming a Fulde-Ferrell-Larkin-Ovchinnikov (FFLO)-like state.^{29,30} It is well known that considering such a large value of α without a finite spin-orbit scattering λ_{so} would cause a first-order transition at low temperatures in the WHH formula, which is often interpreted as a possible realization of the FFLO-like states, contrary to our experimental curve. We chose the value of $\lambda_{so}=1.0$ to avoid this transition and also to produce the best fit for the experimental H_{c2}^{ab} over a broad temperature region, as demonstrated in Fig. 4. The fitting results indicate that a proper value of λ_{so} is essential in determining the shape of the H_{c2}^{ab} curves effectively. Moreover, the presence of a finite λ_{so} enhanced the predicted value of $H_{c2}^{ab}(0)$ over the $H_{c2}^{ab}(0)$ value with $\lambda_{so}=0$ and the same α ; this is consistent with the fact that strong spin-orbit scattering suppresses the Pauli-limiting effect.

On the other hand, for the experimental H_{c2}^c curve, a relatively small $\alpha=1.0$ (dotted line in Fig. 4) was better at describing the H_{c2}^c curve at low temperatures than the $\alpha=0$ case (solid line in Fig. 4), indicating the Pauli-limiting effect exists for both directions. The fit results to the H_{c2}^c data were not very sensitive to variations in λ_{so} from 0 to 3. Because there was no *a priori* reason that the orbital current would experience different spin-orbit scatterings for each crystallo-

graphic direction, we chose the same value of $\lambda_{so}=1.0$ for both H_{c2}^c and H_{c2}^{ab} . The theoretically predicted $H_{c2}(T)$ curves show good agreement with the experimental data over most of the temperature range, except for a small temperature window between 8 and 11 K.

In summary, the presence of the Maki parameter α describing the Pauli-limiting effect in the WHH scheme was essential to describe much smaller $H_{c2}(0)$ values than were expected for the orbital-limiting field. Therefore, the Pauli limiting is postulated to be a dominant mechanism in determining the nearly isotropic $H_{c2}(0)$ behavior because the Zeeman splitting energy should be able to break the singlet Cooper pair in an isotropic manner regardless of details of the electronic structure. In this scenario, a small difference between $H_{c2}(0)$ values for both directions may be due to the presence of small difference in the Landé g factor, causing the Zeeman splitting energy for the two directions to become slightly different. From the ratio of $H_{c2}^{ab}(0)/H_{c2}^c(0)=0.96$, as extrapolated from Fig. 4, g^{ab}/g^c is thought to be about 0.96, which suggests future experimental tests. Furthermore, the results of the fitting, particularly for the H_{c2}^{ab} in Fig. 4, strongly indicate that the existence of spin-orbit scattering in the Fe(Te,Se) system can be a decisive physical process in enhancing the $H_{c2}^{ab}(0)$ beyond the Pauli-limiting field for a weak BCS superconductor ($H_p(0)\equiv 1.86 T_c$) as well as in determining the temperature-dependent evolution of H_{c2} curves at low temperatures.

Having established the importance of the Pauli-limiting effect in iron chalcogenide superconductors, we suspect that nonstoichiometric effects such as those caused by excess Fe or Te(Se) vacancies could be important in enhancing the orbital-limiting field over the Pauli-limiting field. The orbital-limiting field, estimated by the value of $-dH_{c2}/dT$ near T_c , is inversely proportional to the Fermi velocity and the mean free path. According to a recent band calculation for FeSe, the Se vacancy tends to result in a significantly enhanced density of states at the Fermi energy $N(E_F)$ and thus the effective mass.³¹ Moreover, the presence of defects is likely to reduce the mean free path of the system. Both of these effects will lead to an enhanced $-dH_{c2}/dT$ near T_c and, as a result, to enhanced orbital-limiting fields larger than the Pauli-limiting field in the Fe(Te,Se) system. We also note that the $N(E_F)$ of the Fe(Te,Se) system has been found to be relatively large compared with those of other iron pnictides, according to recent first-principles calculations.^{17,32} Therefore, we suggest that either a combination of these two main mechanisms or one of them could be responsible for the manifestation of the Pauli paramagnetic effect in iron chalcogenide superconductors.

Our observations suggest that similar effects may also be equally important for understanding the nearly isotropic $H_{c2}(0)$ behaviors observed in many 122 systems with various dopants and doping levels, although the multiband effect is still needed to properly explain the sublinear increase in H_{c2} curves, particularly near T_c . In light of this, for a more complete description of the H_{c2} curves in various iron pnictides or iron chalcogenides, it may be necessary to consider a

more complete theoretical scheme that includes both the multiband orbital and Pauli paramagnetic effects simultaneously.²⁸

IV. CONCLUSIONS

In summary, we have determined the detailed temperature dependence of upper critical fields in a FeTe_{0.6}Se_{0.4} single crystal by use of a static magnetic field up to 45 T applied along the *ab* plane and the *c* axis. The Pauli paramagnetic effect was clearly evidenced by the flattening in the H_{c2} curves along the *ab* plane and was also indicated by a nearly isotropic $H_{c2}(0) \approx 48$ T in both directions. The enhanced ef-

fective mass and the carrier scattering coming from the excess Fe or Te(Se) vacancies are thought to be responsible for manifesting the Pauli-limiting effect.

ACKNOWLEDGMENTS

This work was supported by the Korean government through National Creative Research Initiatives, GPP (K20702020014-07E0200-01410), and Basic Science Research Programs (2009-0083512). K.H.K. and S.H.K. were supported by LG Yeonam Foundation and Seoul R&BD (10543), respectively. Work at NHMFL was performed under the auspices of the NSF, the state of Florida, and the U.S. DOE.

*khkim@phy.snu.ac.kr

- ¹Y. Kamihara, T. Watanabe, M. Hirano, and H. Hosono, *J. Am. Chem. Soc.* **130**, 3296 (2008).
- ²F. Hunte, J. Jaroszynski, A. Gurevich, D. C. Larbalestier, R. Jin, A. S. Sefat, M. A. McGuire, B. C. Sales, D. K. Christen, and D. Mandrus, *Nature (London)* **453**, 903 (2008).
- ³J. Jaroszynski, F. Hunte, L. Balicas, Y.-j. Jo, I. RaiCevic, A. Gurevich, D. C. Larbalestier, F. F. Balakirev, L. Fang, P. Cheng, Y. Jia, and H. H. Wen, *Phys. Rev. B* **78**, 174523 (2008).
- ⁴Y. J. Jo, J. Jaroszynski, A. Yamamoto, A. Gurevich, S. C. Riggs, G. S. Boebinger, D. Larbalestier, H. H. Wen, N. D. Zhigadlo, S. Katrych, Z. Bukowski, J. Karpinski, R. H. Liu, H. Chen, X. H. Chen, and L. Balicas, *Physica C* **469**, 566 (2009).
- ⁵G. Fuchs, S. L. Drechsler, N. Kozlova, G. Behr, A. Kohler, J. Werner, K. Nenkov, R. Klingeler, J. Hamann-Borrero, C. Hess, A. Kondrat, M. Grobosch, A. Narduzzo, M. Knupfer, J. Freudenberger, B. Buchner, and L. Schultz, *Phys. Rev. Lett.* **101**, 237003 (2008).
- ⁶G. Fuchs, S.-L. Drechsler, N. Kozlova, M. Bartkowiak, J. E. Hamann-Borrero, G. Behr, K. Nenkov, H.-H. Klauss, H. Maeter, A. Amato, H. Luetkens, A. Kwadrin, R. Khasanov, J. Freudenberger, A. Köhler, M. Knupfer, E. Arushanov, H. Rosner, B. Büchner, and L. Schultz, *New J. Phys.* **11**, 075007 (2009).
- ⁷S. A. Baily, Y. Kohama, H. Hiramatsu, B. Maiorov, F. F. Balakirev, M. Hirano, and H. Hosono, *Phys. Rev. Lett.* **102**, 117004 (2009).
- ⁸H.-J. Kim, Y. Liu, Y. S. Oh, S. Khim, I. Kim, G. R. Stewart, and K. H. Kim, *Phys. Rev. B* **79**, 014514 (2009).
- ⁹H. Q. Yuan, J. Singleton, F. F. Balakirev, S. A. Baily, G. F. Chen, J. L. Luo, and N. L. Wang, *Nature (London)* **457**, 565 (2009).
- ¹⁰S. Khim, J. S. Kim, J. W. Kim, S. H. Lee, F. F. Balakirev, Y. Bang, and K. H. Kim, *Physica C* (to be published).
- ¹¹G. F. Chen, Z. G. Chen, J. Dong, W. Z. Hu, G. Li, X. D. Zhang, P. Zheng, J. L. Luo, and N. L. Wang, *Phys. Rev. B* **79**, 140509(R) (2009).
- ¹²M. H. Fang, H. M. Pham, B. Qian, T. J. Liu, E. K. Vehstedt, Y. Liu, L. Spinu, and Z. Q. Mao, *Phys. Rev. B* **78**, 224503 (2008).
- ¹³F.-C. Hsu, J.-Y. Luo, K.-W. Yeh, T.-K. Chen, T.-W. Huang, P. M. Wu, Y.-C. Lee, Y.-L. Huang, Y.-Y. Chu, D.-C. Yan, and M.-K. Wu, *Proc. Natl. Acad. Sci. U.S.A.* **105**, 14262 (2008).
- ¹⁴K.-W. Yeh, T.-W. Huang, Y.-I. Huang, T.-K. Chen, F.-C. Hsu, P. M. Wu, Y.-C. Lee, Y.-Y. Chu, C.-L. Chen, J.-Y. Luo, D.-C. Yan, and M.-K. Wu, *EPL* **84**, 37002 (2008).
- ¹⁵B. C. Sales, A. S. Sefat, M. A. McGuire, R. Y. Jin, D. Mandrus, and Y. Mozharivskyj, *Phys. Rev. B* **79**, 094521 (2009).
- ¹⁶T. J. Liu, B. Qian, D. Fobes, Z. Q. Mao, W. Bao, M. Reehuis, S. A. J. Kimber, K. Prokes, S. Matas, D. N. Argyriou, A. Hiess, A. Rotaru, H. Pham, L. Spinu, Y. Qiu, V. Thampy, A. T. Savici, J. A. Rodriguez, and C. Broholm, *arXiv:1003.5647* (unpublished).
- ¹⁷A. Subedi, L. Zhang, D. J. Singh, and M. H. Du, *Phys. Rev. B* **78**, 134514 (2008).
- ¹⁸Y. Xia, D. Qian, L. Wray, D. Hsieh, G. F. Chen, J. L. Luo, N. L. Wang, and M. Z. Hasan, *Phys. Rev. Lett.* **103**, 037002 (2009).
- ¹⁹T. Kida, T. Matsunaga, M. Hagiwara, Y. Mizuguchi, Y. Takano, and K. Kindo, *J. Phys. Soc. Jpn.* **78**, 113701 (2009).
- ²⁰M. H. Fang, J. H. Yang, F. F. Balakirev, Y. Kohama, J. Singleton, B. Qian, Z. Q. Mao, H. D. Wang, and H. Q. Yuan, *Phys. Rev. B* **81**, 020509(R) (2010).
- ²¹T. J. Liu, X. Ke, B. Qian, J. Hu, D. Fobes, E. K. Vehstedt, H. Pham, J. H. Yang, M. H. Fang, L. Spinu, P. Schiffer, Y. Liu, and Z. Q. Mao, *Phys. Rev. B* **80**, 174509 (2009).
- ²²N. R. Werthamer, E. Helfand, and P. C. Hohenberg, *Phys. Rev.* **147**, 295 (1966).
- ²³B. S. Chandrasekhar, *Appl. Phys. Lett.* **1**, 7 (1962).
- ²⁴A. M. Clogston, *Phys. Rev. Lett.* **9**, 266 (1962).
- ²⁵T. Kato, Y. Mizuguchi, H. Nakamura, T. Machida, H. Sakata, and Y. Takano, *Phys. Rev. B* **80**, 180507 (2009).
- ²⁶T. Hanaguri, S. Nitaka, K. Kuroki, and H. Takagi, *Science* **328**, 474 (2010).
- ²⁷A. Gurevich, *Phys. Rev. B* **67**, 184515 (2003).
- ²⁸A. Gurevich, *Physica C* **456**, 160 (2007).
- ²⁹I. J. Lee, M. J. Naughton, G. M. Danner, and P. M. Chaikin, *Phys. Rev. Lett.* **78**, 3555 (1997).
- ³⁰H. A. Radovan, N. A. Fortune, T. P. Murphy, S. T. Hannahs, E. C. Palm, S. W. Tozer, and D. Hall, *Nature (London)* **425**, 51 (2003).
- ³¹K. W. Lee, V. Pardo, and W. E. Pickett, *Phys. Rev. B* **78**, 174502 (2008).
- ³²L. Zhang, D. J. Singh, and M. H. Du, *Phys. Rev. B* **79**, 012506 (2009).